

# Prediction of flux loss in a Nd-Fe-B ring magnet considering magnetizing process

H Fukunaga<sup>1</sup>, H Koreeda<sup>1</sup>, T Yanai<sup>1</sup>, M Nakano<sup>1</sup> and F Yamashita<sup>2</sup>

<sup>1</sup>Nagasaki University, 14-1 Bunkyo-Machi, Nagasaki, Nagasaki 852-8521, Japan

<sup>2</sup>Minebea Co., Ltd., 1743-1 Asana, Fukuroi, Shizuoka 437-1193, Japan

E-mail: fukunaga@nagasaki-u.ac.jp

**Abstract.** We developed a technique to predict flux loss of a magnet with a complicated magnetization pattern using the finite element method. The developed method consists of four steps. At first, the distribution of magnetization under magnetizing field is analyzed (Step 1), and a demagnetization curve of each element is deduced from the result of the first step (Step 2). After removing the magnetizing field, the distributions of magnetization at room and elevated temperatures are analyzed by using demagnetization curves determined in Step 2 (Step 3). Based on a physical model, the distribution of flux loss due to exposure at the elevated temperature is predicted by using the result obtained in Step 3 (Step 4). We applied this technique to a ring magnet with 10 poles, and large flux loss values were predicted at the transition regions between magnetic poles.

## 1. Introduction

Nd-Fe-B magnets have high remanence and coercivity at room temperature, and have been applied to electrical and electronic devices such as motors. In such applications, a Nd-Fe-B magnet is exposed to an elevated temperature, which causes an irreversible reduction of the flux. This reduction is not recovered even if the magnet is cooled to room temperature, and is called flux loss  $FL$ .  $FL$  is categorized into three types, the permanent, initial, and long-term ones. The three types of  $FL$  originate from metallurgical change, decrease in coercivity, and magnetic aftereffect at an elevated temperature [1]. Generally, the initial flux loss,  $FL_{int}$ , is particularly significant, because it is a large reduction of flux in a short time. As the Curie temperature of  $Nd_2Fe_{14}B$  [2] is much lower than those of  $SmCo_5$  and  $Sm_2Co_{17}$  [3], Nd-Fe-B magnets have a tendency of exhibiting a large  $FL_{int}$  value. Thus, an evaluation of  $FL_{int}$  has increased in importance significantly in many applications.

$FL_{int}$  is affected by local demagnetizing field and its magnitude distributes in a magnet. Thus, a method of predicting  $FL_{int}$  was proposed by some researchers [4, 5]. In that method, however, it is necessary to pre-measure  $FL_{int}$  for magnets with various permeance values, and to obtain the  $FL_{int}$  vs  $\Delta$  curve, where  $\Delta$  is the difference between coercivity and the demagnetizing field. In order to avoid a huge number of pre-measurements, we previously proposed a method of predicting the distribution of  $FL_{int}$  from demagnetizing curves at room and elevated temperatures by taking advantages of the finite element method FEM [6].

In some applications of Nd-Fe-B-based magnets, they are magnetized multi-polarly and  $FL_{int}$  depends on not only local demagnetizing field but also magnetization state of the magnet. In this investigation, we improved the method proposed previously [6] for taking the above effect into account, and proposed a method of predicting  $FL_{int}$  under consideration of magnetizing process.

Subsequently, the developed method was applied to a ring magnet with 10 poles, and the predicted  $FL_{\text{int}}$  was discussed in terms of the magnetization state of the magnet.

## 2. Prediction method of $FL_{\text{int}}$ under consideration of magnetizing process

When the magnet is magnetized in a complicated way, a demagnetization curve depends on the experienced maximum field  $H_m$  and varies from a position to a position in it. For taking this effect into account, we improved the previous method using FEM, took the magnetizing process into account, and set a different demagnetization curve depending on  $H_m$  for each element.

The procedure of the prediction is shown in figure 1. In Step 1, a magnetizing field is applied to a magnet and the distributions of magnetization  $\mathbf{M}$  and magnetic field  $\mathbf{H}$  are simulated by FEM, and a  $H_m$  value for each element is deduced. In Step 2, the corresponding demagnetization curves at room and exposure temperatures are determined for all the elements from the  $H_m$  values obtained in the Step 1 and pre-measured magnetic properties of the magnet. In the Step 3, the magnetizing field is removed, and the distributions of  $\mathbf{M}$  in the magnet at room and exposure temperatures are analyzed by using the demagnetization curves determined in Step 2 with the advantages of FEM. In Step 4, finally, the  $FL_{\text{int}}$  value of each element is reduced from

$$(FL)_{\text{int}} = \frac{1 - I_w(T_{\text{ex}})}{I_w(T_{\text{rt}}) \{1 - \alpha(T_{\text{ex}} - T_{\text{rt}})\}}, \quad (1)$$

where  $I_w(T_{\text{rt}})$  and  $I_w(T_{\text{ex}})$  are the magnetization values of each element at room temperature  $T_{\text{rt}}$  and the exposure temperature  $T_{\text{ex}}$ , respectively, and  $\alpha$  is the temperature coefficient of the remanence. The physical meaning of equation (1) and its validity are reported elsewhere [7,8].

## 3. Pre-measurements of magnetic properties and approximation of demagnetization curve

As magnetic properties depend on  $H_m$  of material, demagnetization curves need to be evaluated at room and exposure temperatures under various values of  $H_m$ . Figure 2 shows an example of evaluation at room temperature. The demagnetization curves of an isotropic Nd-Fe-B bonded magnet were measured with varying  $H_m$  with a vibrating sample magnetometer. Subsequently, the measured coercivity  $H_c$  was approximated as function of  $H_m$  and the flux density  $B$  in the second quadrant were approximated with parabolic function of the applied field  $H$  as

$$B(H) = a_1(H - H_c) + a_2(H - H_c)^2, \quad (2)$$

where  $a_1$  and  $a_2$  are the coefficients of 1st and 2nd order terms, respectively. The values of  $a_1$  and  $a_2$  were determined as an analytical function of  $H_c$  by the least-squares method. As  $H_c$  is approximated as a function of  $H_m$ , we can deduce  $a_1$  and  $a_2$  and resultantly demagnetization curves from  $H_m$ . Similarly, the  $B$  vs.  $H$  curves at an exposure temperature were approximated as a function of  $H_m$ .

The above procedure enables us to deduce the  $B$  vs.  $H$  curves for any value of  $H_m$ . Figure 3 show a

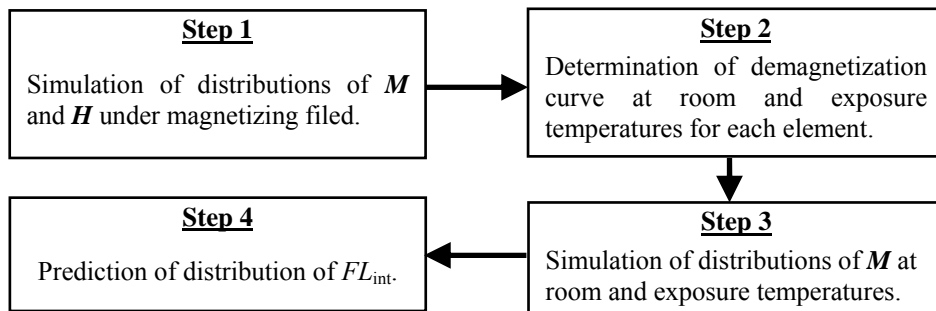


**Figure 1.** Prediction procedure of  $FL_{\text{int}}$  in a magnet under consideration of magnetization process.

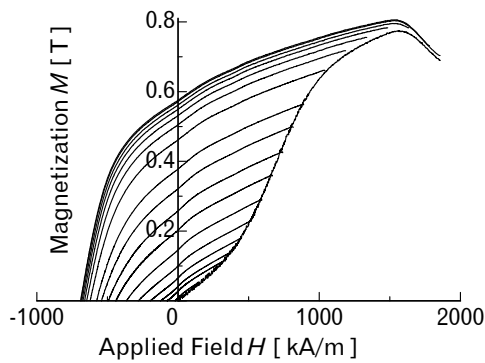


**Figure 2.** Demagnetization curves measured for a Nd-Fe-B bonded magnet with varying maximum applied field.

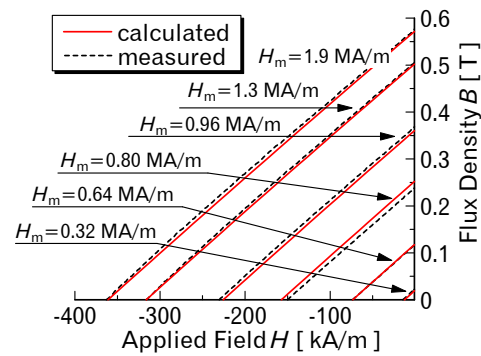


**Figure 3.**  $B$ - $H$  curves deduced for various maximum applied fields at room temperature, together with those obtained by experiments.

comparison of the calculated  $B$  vs.  $H$  curves at the second quadrant with the measured ones for the magnet shown in figure 2. As seen in the figure, the calculated curves fit the experimental ones well, which suggest the validity of the above method.

#### 4. Application of proposed method to a ring magnet

The proposed method was applied to a ring magnet which has isotropic properties indicated in figure 2.

##### 4.1. Detailed Method of prediction

The model ring magnet used in this section is shown in figure 4. The magnet is 25 and 26 mm in inner and outer diameters, respectively, and is covered by an Fe yoke which is 1 mm in thickness.

In Step 1, the magnetizer is located in the magnet as shown in figure 4, and the magnet is magnetized at room temperature so as to have 10 poles by the magnetizing current of 10 kA. Then, we analyzed the distributions of magnetization  $\mathbf{M}$  and magnetic field  $\mathbf{H}$  by using the initial magnetization curve shown in figure 2 with the advantage of FEM. We used a commercially available FEM program (ANSYS), and carried out two-dimensional analysis for one fifth part of the magnet shown by the red arrow in the figure. Consequently,  $H_m$  for each element was determined. Finally, the magnetizer is removed from the magnet.

Based on the analysis of  $H_m$  in Step 1, a  $B$ - $H$  curve for each element was deduced as indicated by equation (2) for room temperature and 120°C. (Step 2). In Step 3, the distributions of  $\mathbf{M}$  are analyzed at room temperature and 120°C by using the  $B$ - $H$  curves determined in Step 2. Finally (Step 4), the  $FL_{int}$  due to exposure at 120 °C in each element was calculated from equation (1).

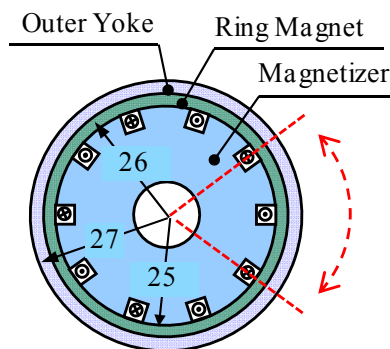


**Figure 4.** Model ring magnet assumed in this investigation. A magnetizer is placed in the magnet in magnetizing process, and is removed before exposure of the magnet at an elevated temperature. The size is indicated in mm.

#### 4.2. Prediction results

Figure 5 shows the distribution of the radial component of magnetization,  $M_n$ , at room temperature after removal of the magnetizer for one tenth part of the magnet corresponding to one pole. Large  $M_n$  values were obtained at the center of the pole and the vicinities of the edges of the conductors. The large  $M_n$  values are attributed to large radial components of magnetizing field in the magnetizing process (Step 1).

The exposure at 120°C causes flux loss, and the distribution of  $M_n$  after exposure is predicted as shown in figure 6 as a function of the electrical angle  $\theta$ . The difference between the solid and broken curves indicates  $FL_{int}$ . The predicted  $FL_{int}$  was large in the vicinities of  $\theta=0$  and  $\pi$  as well as at  $\theta=\pi/6-5\pi/6$ . We should note that local demagnetizing field is low in the vicinities of  $\theta=0$  and  $\pi$ . Thus, the large values in the latter region can be attributed to high local demagnetizing field, and the large  $FL_{int}$  values in the former regions would be explained as follows. As magnetizing field changes its direction at  $\theta=0$  and  $\pi$ ,  $H_c$  against the reversal filed in the radial direction is small in these regions. Therefore, lager  $FL_{int}$  values are expected in these regions even if local demagnetizing field is low.

### 5. Conclusions

The initial flux loss depends on not only local demagnetizing field but also magnetization state of the magnet. For taking the above effect into account, we developed a technique to predict flux loss of a magnet with a complicated magnetization pattern using the finite element method. The developed method was applied to a ring magnet with ten poles, and large flux loss values were predicted at the transition regions between magnetic poles. This result can be explained by small magnetizing filed which the transition regions experienced.

### References

- [1] Clegg A G, Coulson I M, Hilton G and Wong H Y 1990 *IEEE Trans. Magn.* **26** 1492.
- [2] Sagawa M, Fujimura S, Yamamoto H and Matsuura Y 1984 *IEEE Trans. Magn.* **20** 1584.
- [3] Buschow K H J 1988 *Ferromagnetic Materials* vol 1 (Amsterdam, NorthHolland) pp 365-369.
- [4] Itoh K, Hashiba Y, Sakai K and Yagisawa T 1998 *Trans. IEE Jpn.* **118-A** 176 (in Japanese).
- [5] Miyata K 2001 *National Conv. Record IEE Jpn. (Tokyo)* p 2157. (in Japanese)
- [6] Fukunaga H, Toyota A, Mine N and Yamamoto R 2006 *J. Appl. Phys.* **99** 08B525.
- [7] Kanai Y, Hayashida S, Fukunaga H and Yamashita Y 1999 *IEEE Trans. Magn.* **35** 3292 .
- [8] Fukunaga H, Yamamoto R and Yamashita F 2004 *Proc. 18th Int. Workshop on High Performance Magnets and Their Applications (Annecy)* (Annecy) pp 229-235.

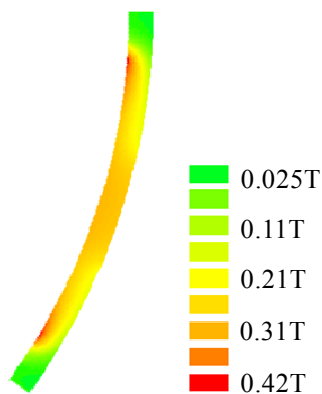


**Figure 5.** Distribution of radial component of magnetization  $M_n$  at room temperature. One tenth part of the magnet is shown.

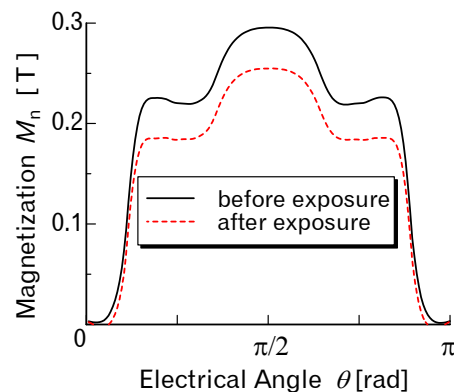


**Figure 6.** Predicted variation of radial component of magnetization due to exposure at 120°C. The value at the centre of the magnet is shown.